Universal Model for Modulated Phases in the Dielectric A_2BX_4 Family

Z. Y. Chen and M. B. Walker
Department of Physics, University of Toronto, Toronto, Ontario, Canada M5S 1A7
(Received 9 April 1990)

A new symmetry-based phenomenological model for the modulated structures in the dielectric A_2BX_4 family is constructed. The model contains a novel competing-interaction mechanism which gives a rich phase diagram. Furthermore, the model gives a universal prediction for both the space groups and the modulation wave vectors for the sequences of phase transitions observed experimentally in the entire A_2BX_4 family.

PACS numbers: 64.60.−i, 64.70.−p, 77.80.Bh

There are two types of theories for modulated structures. A conventional Landau theory[1] accounts for observed symmetries but lacks a single mechanism to produce multiple high-order commensurate (COM) states and "devil's-staircase" phase diagrams (i.e., a different "lock-in" term is required to stabilize each different COM phase[2]). A competing-interaction model, such as the axial next-nearest-neighbor Ising (ANNNI) model[3] or the Janssen-Tjon model,[4] can produce a rich phase diagram for high-order COM states. For example, Janssen[5] has shown that the Janssen-Tjon model can account for many of the observed modulated phases of the A_2BX_4 family; in this model, the stable COM phase of a given wave vector has a unique space-group symmetry, however, whereas more than one space-group symmetry per wave vector has been found to occur experimentally. The current work introduces a new *symmetry-based*, competing-interaction model which has features of both the above and which accounts for both the space-group symmetries and wave vectors of the wide variety of observed modulated phases of the dielectric A_2BX_4 family.[1,6]

The A_2BX_4 family contains a large group of dielectric isostructural crystals having normal phase-space group *Pcmn*. The symbol A represents an alkali-metal ion or equivalent monovalent complex such as NH_4^+ or $(TMA)^+$, i.e., $N(CH_3)_4^+$. The symbol BX_4 represents a divalent tetrahedral complex such as SeO_4^{-2}, $ZnCl_4^{-2}$, or $ZnBr_4^{-2}$. At low temperatures, different but related structure-modulated phases are found as recently reviewed by Cummins.[6] Relevant information for this Letter is summarized in Table I.[6-9] A typical Landau model for these crystals is that of Iizumi *et al.*[10] or Ishibashi,[11] which adequately explains the symmetries of simple low-order COM phases such as those in K_2SeO_4. However, it does not easily account for the high-order COM structures of, say, Rb_2ZnBr_4, or TMA-MCl_4. This is because a lock-in to a COM phase of seventeenth order requires a Landau expansion up to at least the seventeenth order.

The model developed in this Letter has the advantages of both being based on a symmetry analysis (as are conventional Landau theories) and giving rise to the rich phase diagrams characteristic of the competing-interaction models mentioned above.[3,4] Our basic assumptions are that the structures of A_2BX_4 crystals are layered, and that the different layers interact with each other through a *nearest-neighbor* interlayer interaction. The frustrated interaction in our model stems from a nearest-neighbor mixing interaction rather than from a higher-neighbor interaction as in other models.[3,4]

The convention for the unit cell of the basic structure used in this Letter is shown schematically in Fig. 1. The structure can be viewed as being made up of layers per-

TABLE I. Modulated phases observed in the A_2BX_4 family (Refs. 6–9). The commensurate phases are labeled by n/m, where $(n/m)2\pi/c'$ is the wave vector in the extended zone, and by the space groups determined experimentally. In this table INC stands for "incommensurate phase."

Crystals	Wave number n/m (space group)
K_2SeO_4, K_2ZnCl_4, Rb_2ZnCl_4, . . .	Normal → INC → $\frac{1}{3}$ $(Pc2_1n)$
Rb_2ZnBr_4	Normal → INC → $\frac{6}{17}$ → $\frac{1}{3}$ $(Pc2_1n)$ → $\frac{1}{3}$ $(Pc11)$
Cs_2CdBr_4, Cs_2HgBr_4	Normal → INC → $\frac{1}{2}$ $(P112_1/n)$
$(TMA)MCl_4$ (M=Mn, Fe, Zn, Co)	Normal → INC → $\frac{1}{5}$ $(Pc2_1n)$ → (INC) → $\frac{1}{6}$ $(P112_1/n)$ → $\frac{0}{1}$ $(P2_1/c11)$ → $\frac{1}{6}$ $(P2_12_12_1)$ $\searrow$ $\frac{1}{4}$ $(P12_1/c1)$ $\nearrow$
$(NH_4)_2ZnCl_4$	Normal → $\frac{3}{8}$ $(P2_1cn)$ → $\frac{3}{8}$ ($P1c1$ or $P12_1/c1$) → $\frac{1}{3}$ $(Pc2_1n)$
$(NH_4)_2BeF_4$	Normal → INC → $\frac{1}{4}$ $(P2_1cn)$

pendicular to the c axis; the two layers in the unit cell of Fig. 1 are located at levels $z=\frac{1}{4}c$ and $z=\frac{3}{4}c$. All four BX_4 tetrahedra are symmetry related and the A ions with the same greek subscripts are symmetry related also. The symmetry of this structure is described by the orthorhombic space group *Pcmn*. The modulation wave vector is $\mathbf{k}=(0,0,\alpha c^*)$, with $c^*=2\pi/c$.

For a single layer, say, the layer located at $z=c/4$, the two-dimensional space group is generated by $\{E|10\}$, $\{E|01\}$, $\{\sigma_y|0\frac{1}{2}\}$, $\{\sigma_z|\frac{1}{2}\frac{1}{2}\}$, and $\{C_{2x}|\frac{1}{2}0\}$. Symmetry modes are those displacements that transform like basis vectors of a particular irreducible representation (IRREP) of the space group. Here, for simplicity, we discuss only the symmetry modes of the A_α ions for a single layer and their relationship with the three-dimensional symmetry modes called Λ_2 and Λ_3 modes which were shown by Iizumi *et al.*[10] to be the modes producing the modulation of the basic structure in K_2SeO_4. Of the six symmetry modes of the A_α ions for the single layer, we are interested only in the two relevant modes corresponding to IRREP's labeled here as Γ_2 and Γ_3, because only these are directly related to the three-dimensional symmetry modes corresponding to the IRREP's Λ_2 and Λ_3 observed experimentally.[10] These layer modes for the lth layer are

$$e_l(\Gamma_2)=(1,-1),\quad e_l(\Gamma_3)=(1,1)\,, \tag{1}$$

where the first and second entries describe the displacements in the y direction for the $A_\alpha 2$ and $A_\alpha 4$ ions, respectively, for the even l layers, and for the $A_\alpha 1$ and $A_\alpha 3$ ions for the odd l layers. One can show that the three-dimensional symmetry modes Λ_2 and Λ_3 of Ref. 10 can be made up of Bloch-type superpositions of our layer modes Γ_2 and Γ_3. Finally, it should be emphasized that in the Γ_2 and Γ_3 symmetry modes for a layer, all ions in the layer move; it is, however, sufficient for the purpose of characterizing the symmetry of the motion to consider only the A_α ions.

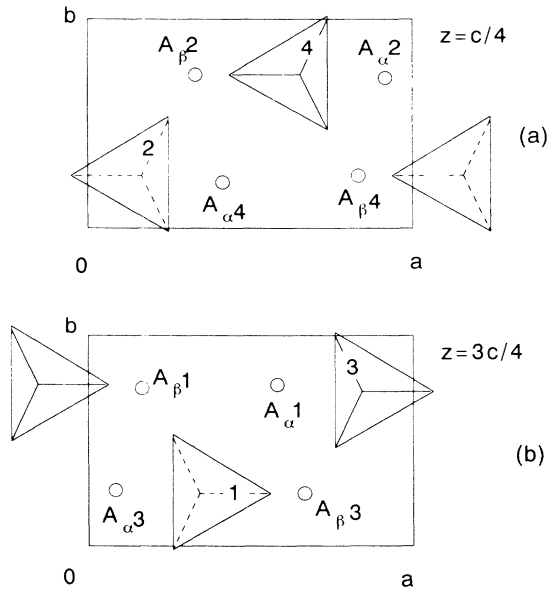

FIG. 1. The structure of A_2BX_4 at its normal phase projected along the c axis. The structure is shown here with two levels at (a) $z=\frac{1}{4}c$ and (b) $z=\frac{3}{4}c$.

The displacements of the A_α ions in layer l are represented by

$$u_l=v_l e_l(\Gamma_2)+w_l e_l(\Gamma_3)\,, \tag{2}$$

where $e_l(\Gamma_2)$ and $e_l(\Gamma_3)$ are the symmetry modes defined in Eq. (1). We take the free energy to be

$$F=\sum_l[\tfrac{1}{2}av_l^2+\tfrac{1}{4}v_l^4+\tfrac{1}{2}a'w_l^2+\tfrac{1}{4}w_l^4+bv_l^2w_l^2]+\tfrac{1}{2}\sum_l(Jv_lv_{l+1}+J'w_lw_{l+1})+\sum_l\tfrac{1}{2}(v_lw_{l+1}-v_{l+1}w_l)\,. \tag{3}$$

This expression is invariant under the transformations of the space group *Pcmn*; also the coefficients of the v_l^4 and w_l^4 terms and of the mixing-interaction term are absorbed into the definitions of the real variables v_l, w_l, and the free energy. There are five undetermined coefficients a, a', b, J, and J' in the free energy (3). The self-interaction term coupling v_l and v_{l+1} favors a ferromagnetic-type profile $(++++)$ for v_l when $J<0$ or an antiferromagnetic-type profile $(+-+-)$ for v_l when $J>0$, where $+$ and $-$ refer to the signs of the variable v_l's. The same situation applies to the w_lw_{l+1} coupling term. The mixing-interaction term coupling v_l with w_{l+1} and v_{l+1} with w_l, however, favors a four-layer period for v_l of the form $(++--)$ while w_l has the form $(+--+)$. There is thus a competition between the self- and the mixing-interaction terms.

The Janssen-Tjon model[4,5] is based on a single-order parameter per layer (corresponding to our v_l) and the frustration mechanism there (a second-neighbor interaction) is thus different from ours. Experimental studies[10] of the soft mode in K_2SeO_4 indicate that the Γ_2 and Γ_3 contributions are comparable in magnitude, and this gives an experimental basis for including two-order parameters per layer (v_l and w_l) as we do.

Although the model of Eq. (3) appears one dimensional, it is effectively three dimensional since v_l and w_l characterize an entire two-dimensional layer. Thus our mean-field treatment is a reasonable approximation.

Introducing Fourier transforms of the variables v_l and w_l and diagonalizing the effective dynamical matrix, we find that the two branches of the dispersion curve for the high-temperature normal phase are given by

$$\omega_\pm^2(k)=\tfrac{1}{2}\{a_++J_+\cos kc' \pm[(a_-+J_-\cos kc')^2+\sin^2kc']^{1/2}\}\,, \tag{4}$$

where we have defined $a_{\pm}=\frac{1}{2}(a\pm a')$ and $J_{\pm}=\frac{1}{2}(J\pm J')$. The branch $\omega_{-}^{2}(k)$ is always lower than $\omega_{+}^{2}(k)$. The mixing-interaction term in (3) for v_l and w_{l+1} is crucial for producing a minimum in the dispersion curves at an arbitrary incommensurate (INC) k_m whose value is a function of the system-dependent parameters, and is thus a function of, e.g., temperature and pressure. When the temperature is lowered from the normal phase, the minimum of the dispersion curve $\omega_{-}^{2}(k)$ goes to zero at the normal-INC transition temperature, and the system undergoes a phase transition to a modulated structure with a wave vector k_m.

To obtain the phase diagram for the free energy (3), a numerical analysis has been conducted. The procedure is similar to that of other competing-interaction models.[3,4] The minimization conditions $\partial F/\partial v_l=\partial F/\partial w_l=0$ were solved numerically. In addition, the boundary conditions $v_{l+m}=v_l$ and $w_{l+m}=w_l$ are imposed. This yields

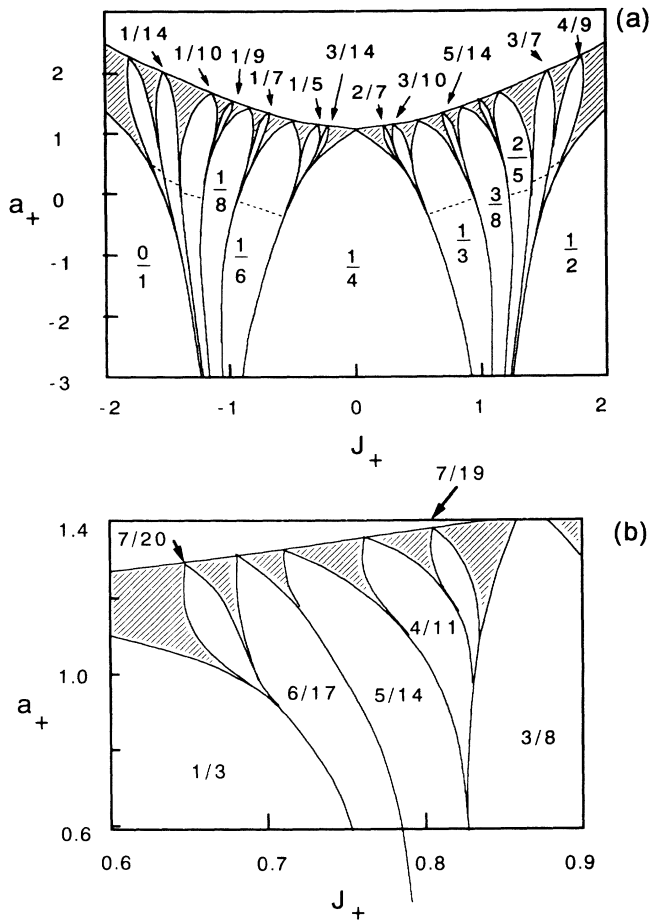

FIG. 2. The phase diagrams produced from our model using $b=0$, $a_{-}=0.4$, and $J_{-}=0$. The space-group symmetries are listed in Table II. The commensurate phases are labeled by n/m, where $(n/m)2\pi/c'$ is the wave vector. The shaded areas indicate higher-order COM or INC regions. (a) A global phase diagram with m up to 10. (b) An exploded phase diagram near the $\frac{1}{3}$ phase with m up to 20.

COM phases characterized by COM wave vectors[12] $k=(n/m)c'^{*}$, where the ratio n/m is irreducible with n and m integers, and $c'^{*}=2\pi/c'$ with $c'=c/2$ the interlayer distance. We have arbitrarily chosen parameters $J_{-}=b=0$ and $a_{-}=0.4$ to produce the phase diagrams shown in Fig. 2. To obtain Fig. 2(a), values of m from 1 to 10 were considered; Fig. 2(b) is an exploded phase diagram for the region between the $\frac{1}{3}$ and $\frac{3}{8}$ phases with values of m up to 20 considered. The shaded areas indicate higher-order COM or INC regions. We can determine the space-group symmetry from the profile of the variables v_l and w_l using Eqs. (1) and (2). For each phase, we have studied the behavior of the profile of the parameters v_l and w_l. At low a_{+}, the profile of the order parameter implies a structure that has low-temperature symmetry listed in Table II. The space groups listed here are consistent with those allowed for the symmetry considerations of Janssen.[5] For wave vector [odd/(2 $\times$even)]c'^{*}, this symmetry remains valid all the way to the normal-COM transition line. For other wave vectors, there is a phase transition to a phase having the same wave vector but a different symmetry when a_{+} increases. This phase transition, represented by dashed curves in Fig. 2, corresponds to a transition from a phase with both ω_{+} and ω_{-} modes to a phase with an ω_{-}-only mode. The ω_{-}-only model is the one that yields the structures which have the most-often observed symmetry in the A_2BX_4 family. For this mode, there is a special symmetry for the profile of v_l and w_l. For example, when $n/m=n/\text{odd}$, v_l is an odd function of $l-\frac{1}{2}$ while w_l is an even one. Also, we note that if one replaces a_{-} with $-a_{-}$, the phase diagram in Fig. 2 is not changed but the profiles for v_l and w_l are interchanged, and thus the space group is different for $a_{-}<0$.

The phase diagram in Fig. 2 and the corresponding space-group symmetries in Table II agree with the experimental results in Table I. The first group of compounds, represented by K_2SeO_4,[6] initially goes through a normal-INC phase transition, and then undergoes an INC-COM phase transition. The resultant COM phase $\frac{1}{3}$ has the space group $Pc2_1n$ corresponding to the $a_{-}>0$ case in our model, as in Table II. The crystal Rb_2ZnBr_4 also belongs to this group but an interesting $\frac{6}{17}$ phase is observed between the INC phase and the COM $\frac{1}{3}$ phase.[6,8] The crystal Rb_2ZnBr_4 also displays a

TABLE II. Space groups determined from our model for phases in Fig. 2.

n/m	High a_{+} ($a_{-}>0$)	High a_{+} ($a_{-}<0$)	Low a_{+}
odd/(2$\times$odd)	$P112_1/n$	$P2_12_12_1$	$P112_1$
n/odd	$Pc2_1n$	$P2_1/c11$	$Pc11$
odd/(2$\times$even) (low b)	$P12_1/c1$	$P12_1/c1$	$P12_1/c1$
odd/(2$\times$even) (high b)	$P2_1cn$	$P2_1cn$	$P2_1cn$

phase transition from the $\frac{1}{3}$ ($Pc2_1n$) phase to a $\frac{1}{3}$ ($Pc11$) phase corresponding to the low-a_+ case. The second group is Cs_2CdBr_4 and Cs_2HgBr_4.[6,9] This group undergoes phase transitions from the normal phase to an INC phase, then to a COM phase. This COM phase corresponds to the zone center mode of the IRREP Λ_2, which has $n/m=1/2$ here.[12] The experimentally observed space group is $P112_1/n$ which is consistent with our model as indicated in Table II. The third group consists of a large group of crystals[6] commonly denoted (TMA)MX_4 (where M=Mn, Fe, Zn, Co, X=Cl, Br). Under zero pressure, the Fe, Zn, and Co salts first go through a normal-INC phase transition, then a INC-COM phase transition to a $\frac{1}{5}$ COM phase with space group $Pc2_1n$. As the temperature is further lowered, they undergo phase transitions to a $\frac{1}{6}$ COM phase with space group $P112_1/n$, through a possible intermediate INC phase. These transitions can be well explained by our model as in Table II, corresponding to $a_- > 0$. When the temperature is further lowered, these crystals undergo COM-COM phase transitions to a $\frac{0}{1}$ COM phase with space group $P2_1/c$.[6] From this phase they experience a reentrant phase transition to the $\frac{1}{6}$ COM phase but with a space group $P2_12_12_1$. These two COM-COM phase transitions can also be qualitatively explained by our model. We assume that when the transition from the first $\frac{1}{6}$ phase to the $\frac{0}{1}$ phase takes place, the parameter a_- changes sign. According to Table II, the $\frac{0}{1}$ phase thus has the space group $P2_1/c11$. When the reentrant transition occurs, the $\frac{1}{6}$ phase should have the space group $P2_12_12_1$ for $a_- < 0$. The Mn salt is somewhat different from the others. Instead of the $\frac{1}{5}$ phase, a $\frac{1}{4}$ ($P12_1/c1$) COM phase is stable between the INC and the $\frac{1}{6}$ phase. The sequence of phase transitions of Mn salt can also be explained by our model.

So far we have let $b=0$. When b increases, we also found that, for wave vector [odd/(2×even)]c'^*, a phase transition occurs from the phase having $P12_1/c1$ symmetry to a phase having the same wave vector but the symmetry $P2_1cn$. This prediction is consistent with experimental observations of the last group in the A_2BX_4 family. The crystal $(NH_4)_2ZnCl_4$ undergoes a normal-COM phase transition to a $\frac{3}{8}$ COM phase with a space group $P2_1cn$ (high-b case); when b decreases, it undergoes a COM-COM phase transition to a phase characterized by the same wave vector $\frac{3}{8}$ but with a different space group $P12_1/c1$ (low-b case); furthermore, it undergoes a COM-COM phase transition to the $\frac{1}{3}$ COM phase with the space group $Pc2_1n$ as shown in Fig. 2 and Table II. The crystals $(NH_4)_2BeF_4$ and $(ND_4)_2BeF_4$ first undergo a normal-INC phase transition and then a first-order INC-COM phase transition to a $\frac{1}{4}$ phase of the high-b symmetry $P2_1cn$. This is also consistent with our model.

In conclusion, we note that the novel competing-interaction model which arose in this Letter from a study of the A_2BX_4 family of compounds has provided a basis for understanding the remarkably diverse series of phase transitions and space-group symmetries which occur in these materials.

We wish to acknowledge helpful comments from A. E. Jacobs and the support from the Natural Sciences and Engineering Research Council of Canada.

[1]R. Blinc and A. P. Levanyuk, *Incommensurate Phases in Dielectrics* (North-Holland, Amsterdam, 1986), Vols. 1 and 2.

[2]K. Parlinski and F. Dénoyer, J. Phys. C **18**, 293 (1985).

[3]P. Bak and J. von Boehm, Phys. Rev. B **21**, 5297 (1980); Y. Yamada and N. Hamaya, J. Phys. Soc. Jpn. **52**, 3466 (1983); for a recent review, see W. Selke, Phys. Rep. **170**, 213 (1988).

[4]T. Janssen and J. A. Tjon, Phys. Rev. B **24**, 2245 (1981); **25**, 3767 (1982).

[5]T. Janssen, Ferroelectrics **66**, 203 (1986).

[6]H. Z. Cummins, Phys. Rep. **185**, 211 (1990), and references therein.

[7]A. Hedoux and D. Grebille, Acta Crystallogr. Sect. B **45**, 370 (1989).

[8]A. C. R. Hogervorst and R. B. Helmholdt, Acta Crystallogr. Sect. B **44**, 120 (1988).

[9]N. L. Spezial and G. Chapuis, Acta Crystallogr. Sect. B **45**, 20 (1989).

[10]M. Iizumi, J. D. Axe, G. Shirane, and K. Shimaoka, Phys. Rev. B **15**, 4392 (1977).

[11]Y. Ishibashi, in Ref. 1, Vol. 2.

[12]Here k corresponds to the extended zone wave vector of Ref. 4. The Λ_2 and Λ_3 modes of Ref. 4 are characterized by reduced zone wave vectors $k_r=c^*-k$ and $k_r=k$, respectively.